

PAPER • OPEN ACCESS

CFD analysis of texture depth effect on the performance of hydrodynamic lubricated bearing

To cite this article: M Muchammad *et al* 2018 *J. Phys.: Conf. Ser.* **1090** 012067

View the [article online](#) for updates and enhancements.



IOP | ebooks™

Bringing you innovative digital publishing with leading voices to create your essential collection of books in STEM research.

Start exploring the collection - download the first chapter of every title for free.

CFD analysis of texture depth effect on the performance of hydrodynamic lubricated bearing

M Muchammad^{1,2*}, F Hilmy¹, M Tauviqirrahman¹, J Jamari¹, DJ Schipper²

¹Laboratory for Engineering Design and Tribology, Mechanical Engineering Department, Diponegoro University, Indonesia.

²Laboratory for Surface Technology and Tribology, Faculty of Engineering Technology, University of Twente, The Netherlands.

m_mad5373@yahoo.com

Abstract. Surface modification of the lubricated bearing such texturing has proven to improve the hydrodynamic performance. The present paper examined the effect of texture depth as well as the texture length on the tribological performance using computational fluid dynamic (CFD) approach. The cavitation model was also considered to obtain more realistic characteristic of bearing. It was shown that by increasing texture depth of the surface of bearing, the enhanced hydrodynamic pressure was achieved. Moreover, other interesting result is that the length of cavitation region decreases with the increase in texture depth and the decrease in texture length.

1. Introduction

For more decades, the research of texturing of the lubricated contact has obtained an explosion interest by researchers around the world. It is well known that texturing technique has proven to improve the lubrication characteristics. Numerous researchers based on hydrodynamic lubrication theory have introduced several mechanisms of lift generation of textured surfaces.

Fowell et al. [1] using a mass-conserving numerical analysis concluded that any convergence between the bearing surfaces provides a significant mechanism for lift generation. Gherca et al. [2] evaluated the effects of the texture geometry using a mass-conserving model. It was found that the load support was strongly dependent on the geometrical features such as size, density, and shape. Henry et al. [3] experimentally studied the effect of surface texturing on the steady-state behavior of bearings. They concluded that the textured bearings reduces friction up to 30% at low loads while for heavy loads, their performance is equivalent or even lower than that of an untextured bearing. Yagi et al. [4] studied the value of the load support enabled by textured pattern in hydrodynamic lubrication regime. They concluded that the mechanism of lift generation was strongly affected by boundary condition. Zhang et al. [5] investigated the effect a rectangular array of circle dimples on the film thickness profile. It was concluded that the lift generation could be improved through appropriate partial arrangement of textures. Later, Shinde and Pawar [6] proposed the optimal surface texturing parameters to improve performance of bearing.

Based on published works, it can be highlighted that texturing produces more positive effect compared to pure texturing with respect to the load support. However, from literature survey, most of the solution of the lubrication problems have been solved by of Reynolds equation which may be questionable in particular cases with low viscosity and high runner velocities.



Following this main frame, in the present paper a CFD method as well as the Reynolds equation have been applied to investigate the texturing parameter in particular case of texture depth on the hydrodynamic pressure. For obtain more accurate results, the cavitation model is also considered.

2. Methodology

2.1. Theory

In the present study, the lubrication problem is solved by the Navier-Stokes equation and continuity equations. The Navier-Stokes (N-S) equations are solved over the domain using a finite-volume method with the commercial CFD software package FLUENT®. The Navier-Stokes and the continuity equations can be expressed, respectively.

$$\rho \frac{Du_i}{Dt} = -\frac{\partial p}{\partial x_i} + \rho G_i + \frac{\partial}{\partial x_j} \left[2\eta e_{ij} - \frac{2}{3}\eta(\nabla \cdot u_i)\delta_{ij} \right] \quad (1)$$

$$\nabla \cdot u = 0 \quad (2)$$

Not like the previously published works in which the cavitation model is ignored, in the present study, the cavitation effect is taken into account. In FLUENT®, there are three available cavitation models: Schneer and Sauer model, Zwart-Gelber-Belamri model and Sighal et al. model [7]. In this study, the Zwart-Gelber-Belamri is employed due to their capability (less sensitive to mesh density, robust and converge quickly [7]).

In addition to the Navier-Stokes equation, in this work, the lubrication problem is also solved by modified Reynolds equation (Eq. 3 as below). For more detail, the derivation of such equation used here is described in [8, 9]. It should be noted that the isoviscous Newtonian one-dimensional Reynolds equation with slip is derived from a simple of the x-component of the Navier-Stokes equation that assumes an incompressible flow, neglecting the inertia effects in the film. However, for the analysis studied here, the slip coefficient is set to zero.

$$P_2 \left[\left(h_p^3 + 3h_p^3 K_p \right) \frac{ab+bc}{ab^2} + \left(\frac{h_0^3 + 3h_0^3 K_0}{a} \right) \right] = P_{atm} \left[\left(h_p^3 + 3h_p^3 K_p \right) \frac{ab+bc}{ab^2} + \left(\frac{h_0^3 + 3h_0^3 K_0}{a} \right) \right] - 6\mu U \left[\left(h_p + h_p K_p \right) - \left(h_0 + h_0 K_0 \right) \right] \quad (3)$$

2.2. CFD Model

Figure 1 gives the schematic illustration of a parallel textured (pocketed) sliding bearing. The assumption of the no-slip is adopted. The main characteristics of the bearing and the lubricant properties studied are presented in Table 1 and 2 respectively.

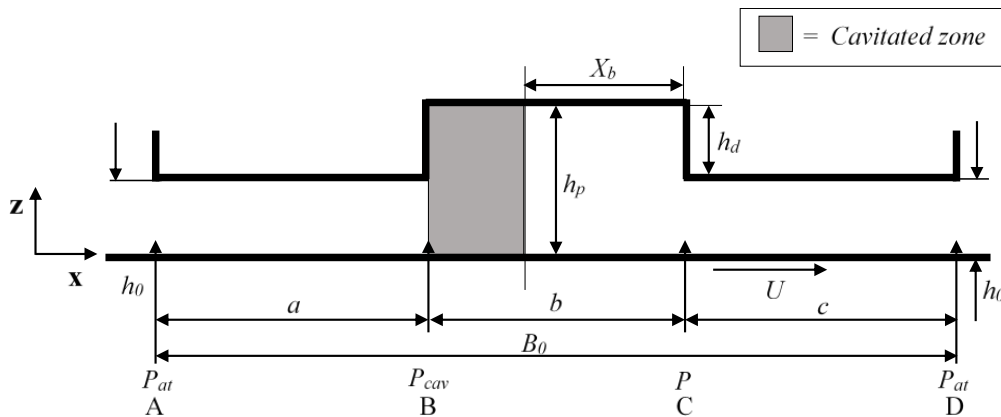


Figure 1. Geometry of slider bearing 2D model.

Table 1. Characteristics of main parameter bearing analyzed.

Parameter	Symbol	Value	Unit
Length of bearing	B_o	2.00	mm
Length of inlet	a	0.75	mm
Length of texture	b	0.50	mm
Length of outlet	c	0.75	mm
Minimum film thickness	h_o	4.00	μm
Depth of texture	h_d	2.00 ; 8.00	μm
Inlet pressure	P_a	100	kPa
Cavitation pressure	P_c	50	kPa
Sliding velocity	U	1	m/s

Table-2. Characteristics of lubricant properties.

Parameter	Symbol	Oil	Oil Vapor	Unit
Density	ρ	962	0.02556	kg/m^3
Viscosity	μ	0.013468	1.256×10^{-5}	kg/ms

In the present study, the grid consists of three blocks with grid system as shown in Fig. 2. The number of grids in the longitudinal direction (N_x) and transverse (N_z) is 1000 x 100. These grids results in 90,000 cells, faces 18,112 and 91,121 nodes based on the independent mesh study.

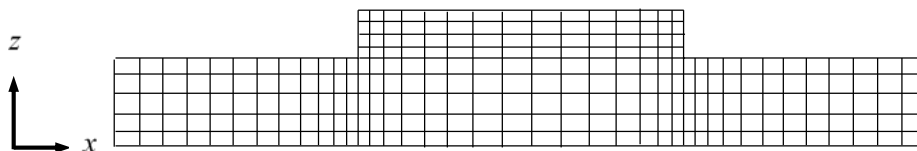


Figure 2. Grid system analyzed in numerical analysis.

In the present work, the texture depth is of particular interest. The pocket depth is categorized to two kinds, that is, low texture depth and high texture depth, as shown in Fig. 3. The hydrodynamic pressure

is used as indicator to describe the texture depth effect with respect to the Reynolds equation and Navier-Stokes equation..



Figure 3. Pocket depth analyzed (a) $h_d = \frac{1}{2} h_o$ (low texture depth), (b) $h_d = 2 h_o$ (high texture depth).

3. Result and discussion

In this section, the results of the application of different texture depths with respect to pressure distribution graph are shown. In Fig. 4, the pressure distribution with $b = 0.25$ at low and high texture depth is presented. It can be observed from Fig. 4a that the N-S solution gives a larger prediction of pressure compared to Reynolds approach for low texture depth. It indicates that the inertia effect exists in the case of low texture depth. As a note, this inertia term cannot be predicted by Reynolds equation. The interesting finding is that when texture depth is increased, the inertia effect has gone. As indicated in Fig. 14b, the prediction of the hydrodynamic pressure by the N-S equation and the Reynolds approach is exactly the same.

Related to the cavitation behavior, textured contact with low texture depth leads to the generation of the cavitation area. However, the N-S equation tends to predict the cavitation area smaller than the Reynolds approach. On the other hands, the Reynolds theory underestimates the hydrodynamic pressure when the inertia effect has a dominant role in the texture contact.

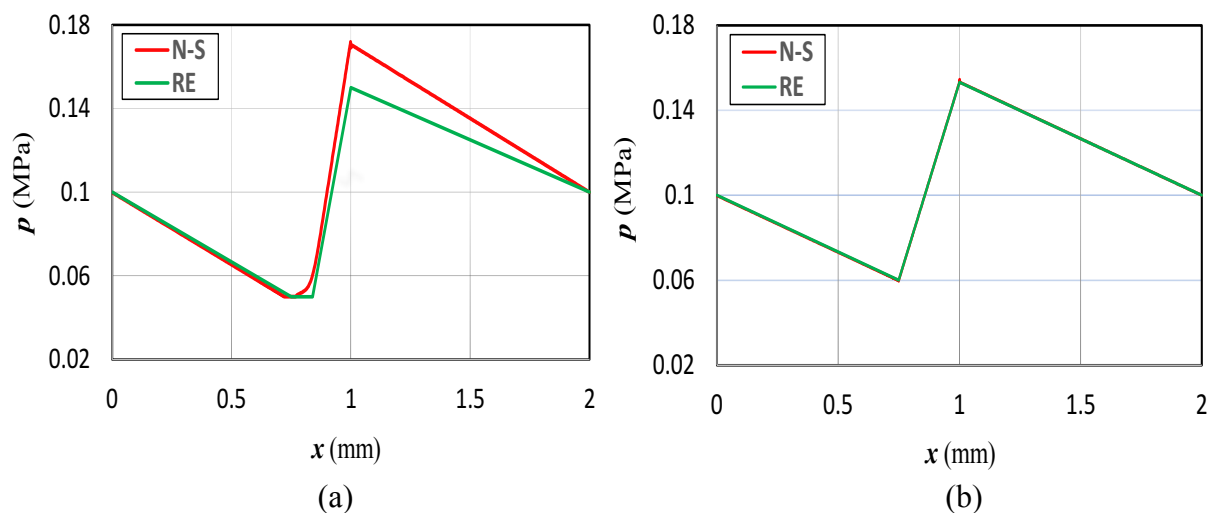


Figure 4. The pressure distribution as a function of coordinate in sliding direction (a) low texture depth, and (b) high texture depth, of interest with $b = 0.25$ mm.

Figure 5 shows the hydrodynamic pressure predicted by the N-S approach and the Reynolds equation for the case of length of contact $b = 0.5$ mm. It can be seen that for the case of high texture depth, the pressure distribution predicted by the N-S approach is larger than the Reynolds equation. It means that the inertia effect exists in the texture contact with larger length of contact b . For low texture depth, the

prediction of the pressure by two approaches is the same, in particular to the cavitation region. On the other words, the inertia and the cavitation term is independent. The profile of the hydrodynamic pressure is strongly affected by the texture depth as well as the texture length. This finding is strengthened by the simulation result as indicated in Figure 6. For high b , in this case $b = 0.75$, the prediction by two approaches is similar both for low and high texture depth.

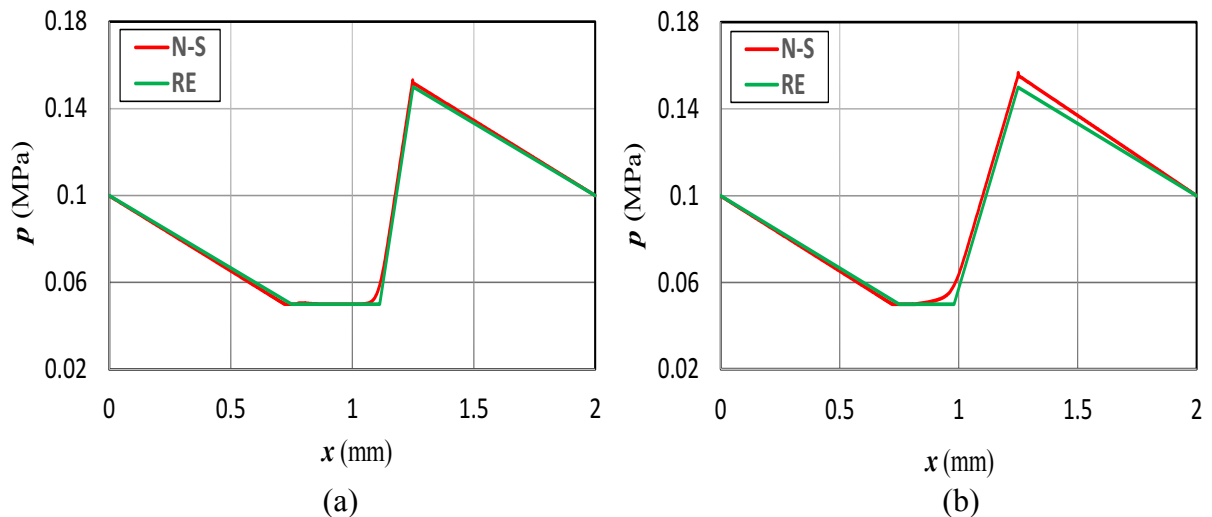


Figure 5. The pressure distribution as a function of coordinate in sliding direction (a) low texture depth, (b) high texture depth, of interest with $b = 0.5$ mm.

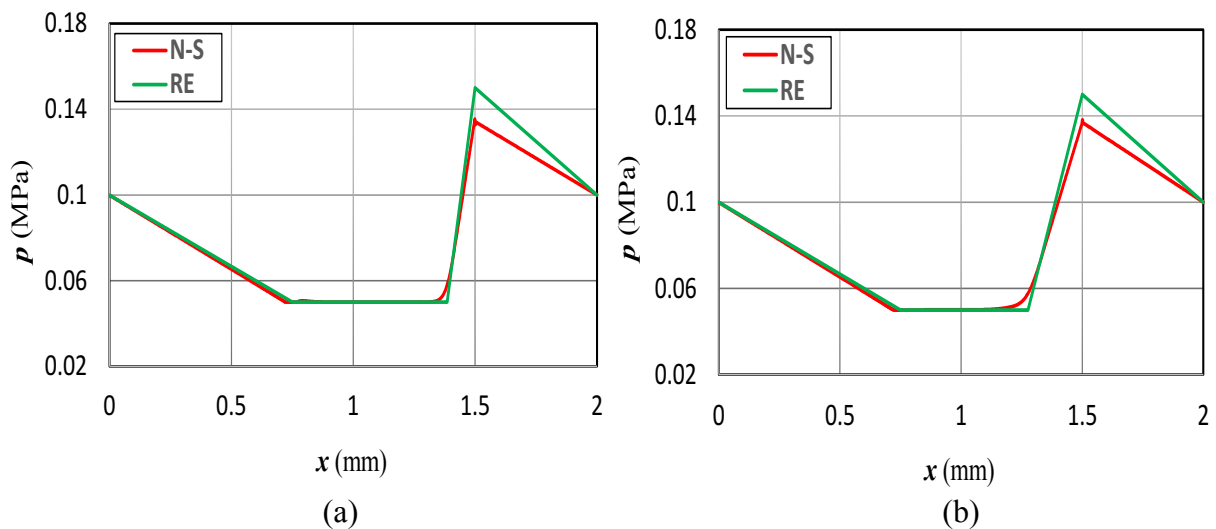


Figure 6. The pressure distribution as a function of coordinate in sliding direction (a) low texture depth, (b) high texture depth, of interest with $b = 0.75$ mm.

Figure 7 shows the load support for each texture depth and bearing texture length configuration, either obtained by the CFD method with the Navier-Stokes equation or by the Reynolds equation method. In general, load support decreases with increasing texture length and increases with increasing texture depth except for the case of high texture depth with texture length of 0.25 mm. Under these conditions the support load decreases. A part from that phenomenon, generally the high texture depth gives a positive effect on bearing performance. This is influenced by the higher cavitation region at large texture length. Conversely, a high texture depth actually makes the cavitation region smaller. This

indicates that the occurrence of cavitation causes a negative effect on bearing performance. Thus, this study indicates that the maximum bearing performance corresponds to the smallest texture length configuration of 0.25 mm with low texture depth.

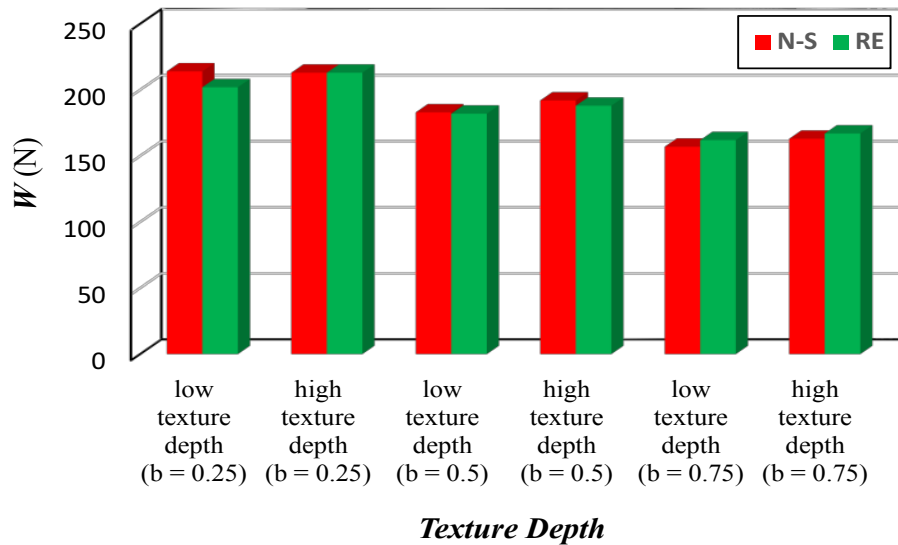


Figure 7. The load support as a function of texture depth.

4. Conclusions

In the present study, the lubrication analysis of the single textured contact was solved by two approaches; the Navier-Stokes Equation and the Reynolds equation. Based on the explanation discussed earlier, the conclusion can be drawn as follows:

1. The increasing texture depth leads to the enhanced of the hydrodynamic pressure.
2. The increasing texture depth decreases the cavitation area.
3. The decreasing texture length decreases the cavitation area.

References

- [1] Fowell M T, Medina S, Olver A V, Spikes H A, Pegg I G 2012 *Tribol. Int.* **52** 7
- [2] Gherca A R, Maspeyrot P, Hajjam M, Fatu A 2013 *Tribol. Trans.* **56(3)** 321
- [3] Henry Y, Bouyer J, Fillon M 2015 *Proc. Instn. Mech. Eng. Part J: J. of Eng. Tribology* **229(4)** 362
- [4] Yagi K, Sato H, Sugimura J 2015 *Tribol. Online* **10(3)** 232
- [5] Zhang H, Dong G, Hua M, Guo F, Chin K S 2015 *Ind. Lubr. Tribol.* **67(4)** 359
- [6] Shinde A B, Pawar P M 2017 *Tribol. Int.* **144** 349
- [7] ANSYS, ANSYS Fluent, version 14.0: user manual. ANSYS, Inc., Canonsburg, USA., 2011
- [8] Muchammad M, Tauviqirrahman M, Jamari J, Schipper D J 2017 *Lubr. Sci.* **29(3)** 133
- [9] Muchammad M, Tauviqirrahman M, Pratomo A W, Jamari J, Schipper D J 2017 *IJSurfSE* **11(2)** 100